Orientation-dependent transport in junctions formed by d-wave altermagnets and d-wave superconductors

Wenjun Zhao [1], Yuri Fukaya [2], Pablo Burset [3,4,5], Jorge Cayao [6], Yukio Tanaka [7], and Bo Lu [1]

[1] *Center for Joint Quantum Studies, Tianjin Key Laboratory of Low Dimensional Materials Physics and Preparing Technology, Department of Physics, Tianjin University, Tianjin 300354, China*
[2] *Faculty of Environmental Life, Natural Science and Technology, Okayama University, 700-8530 Okayama, Japan*
[3] *Department of Theoretical Condensed Matter Physics, Universidad Autónoma de Madrid, 28049 Madrid, Spain*
[4] *Condensed Matter Physics Center (IFIMAC), Universidad Autónoma de Madrid, 28049 Madrid, Spain*
[5] *Instituto Nicolás Cabrera, Universidad Autónoma de Madrid, 28049 Madrid, Spain*
[6] *Department of Physics and Astronomy, Uppsala University, Box 516, S-751 20 Uppsala, Sweden*
[7] *Department of Applied Physics, Nagoya University, Nagoya 464-8603, Japan*

(Received 3 February 2025; accepted 29 April 2025; published 16 May 2025)

We investigate de Gennes-Saint-James states and Josephson effect in hybrid junctions based on d-wave altermagnet and d-wave superconductor. Even though these states are associated to long junctions, we find that the $d_{x^2-y^2}$ altermagnet in a normal metal/altermagnet/d-wave superconductor junction forms de Gennes-Saint-James states in a short junction due to an enhanced mismatch between electron and hole wave vectors. As a result, the zero-bias conductance peak vanishes and pronounced resonance spikes emerge in the subgap conductance spectra. By contrast, the d_{xy} altermagnet only features de Gennes-Saint-James states in the long junction. Moreover, the well-known features such as V-shape conductance for $d_{x^2-y^2}$ pairings and zero-biased conductance peak for d_{xy} pairings are not affected by the strength of d_{xy} altermagnetism in the short junction. We also study the Josephson current-phase relation $I(\varphi)$ of d-wave superconductor/altermagnet/d-wave superconductor hybrids, where φ is the macroscopic phase difference between two d-wave superconductors. In symmetric junctions, we obtain anomalous current phase relation such as a 0-π transition by changing either the orientation or the magnitude of the altermagnetic order parameter and dominant higher Josephson harmonics. Interestingly, we find the first-order Josephson coupling in an asymmetric $d_{x^2-y^2}$-superconductor/altermagnet/d_{xy}-superconductor junction when the symmetry of altermagnetic order parameter is neither $d_{x^2-y^2}$ nor d_{xy} wave. We present the symmetry analysis and conclude that the anomalous orientation-dependent current-phase relations are ascribed to the peculiar feature of the altermagnetic spin-splitting field.

DOI: 10.1103/PhysRevB.111.184515

I. INTRODUCTION

Heterostructures formed by superconductors coupled to normal state materials bear a great interest in condensed matter physics due to their potential for realizing emergent superconducting phenomena of use for future quantum applications [1–5]. These novel states are often characterized by low-energy excitations within the superconducting gap, or subgap states, that can be controlled with great precision. In the simplest case, when a finite size normal metal is in contact with a superconductor, subgap bound states appear in the normal region known as de Gennes-Saint-James states [6] which are also called Andreev bound states [7,8]. According to Bohr-Sommerfeld quantization [9], these states form when the total accumulation of phase becomes a multiple of 2π during a complete cycle comprising two Andreev reflections at the normal metal-superconductor interface and two normal reflections at the open edge of the normal metal. The bound states manifest themselves as a series of pronounced conductance spikes [10] which have been observed experimentally in various metallic materials backed on one side by a superconductor [11,12]. The spikes oscillate as a function of the thickness of the normal region with characteristic length $\xi_S = \hbar v_F/(\pi\Delta)$, where Δ is the superconducting gap. Notably, with unconventional pairing states, such as d-wave pairings, the resonant bound states evolve into flat zero-energy surface Andreev bound states [13–16] and can be found at normal regions of arbitrary thickness [17,18]. The surface flat bands manifest themselves as a zero bias conductance peak in tunneling spectroscopy [14,17,19–23].

The de Gennes-Saint-James states have also been extensively studied in ferromagnet/superconductor hybrids [24–29]. In this regard, it was shown that the oscillations at the scale of ξ_F in the induced pairing amplitude and in the local density of states at the Fermi energy are related to the evolution of the resonant states [25], where $\xi_F = \hbar v_F/(\pi M)$ is the ferromagnetic coherence length with M the exchange field in the ferromagnet. Here, ξ_F is generally much smaller than ξ_S so that the oscillation is short ranged. For strong ferromagnets such as half metals, Andreev reflection is often suppressed or forbidden [30–32]. Remarkably, equal spin Andreev reflection was observed in experiments due to spin-flip and spin-mixing processes at the spin-active boundary

 ©2025 American Physical Society

between ferromagnet and superconductor [33], and is the key factor to produce the resonant states in the superconducting gap.

Recently, a novel class of magnets dubbed altermagnets (AMs) has attracted substantial interest [34–50]. AM materials exhibit anisotropic nonrelativistic introin splitting field, without net magnetization. From symmetry perspective, the opposite-spin sublattices in AMs are connected by rotational or mirror symmetries, rather than translational or inversion symmetries, leading to even-parity order parameter such as d, g wave, etc. Various AM materials have been found like RuO_2 [36,38,42], MnTe [51–53], and FeS [54], see also Refs. [43,45,48].

The interplay between altermagnetism and superconductivity bears fundamental interest and is expected to be useful for spintronic applications [50]. It was found that the Andreev reflection in AM/superconductor (SC) junctions is strongly orientation dependent [55–59] and spin polarized [60]. Also, it was shown that even without net magnetization, there are 0-π oscillations when modulating the junction length and AM strength in Josephson junctions with spin-singlet SCs and d-wave AMs [61–63]. The exotic φ-Josephson junction was also predicted in altermagnetic Josephson junctions with simplest s-wave pairing potential [64,65]. It was shown that the current-phase relation has a rich diversity of anomalous characteristics such as multiple nodes [64], tunable skewness [66], and orientation dependence [67]. Despite the recent efforts, transport in junctions formed by AMs and high-temperature superconductors has so far received little attention. Given that d-wave AMs represent the magnetic counterparts of high-temperature superconductor with d-wave pairings, it is natural to wonder about transport in junctions formed by them. This problem, however, has not been addressed yet.

In this paper, we focus on the transport characteristics in two types of hybrid junctions combining d-wave superconductors (d-SCs) and a d-AM interlayer. First, we study the normal metal (N)/AM/d-SC junction as depicted in Fig. 1(a). We investigate the possibility of the formation of de Gennes-Saint-James states and the robustness of the zero-energy surface Andreev bound states against altermagnetic order. We demonstrate the schematics of the quasiparticle trajectories in Fig. 1(c) with four modes to form resonant states, which are depicted in Figs. 1(d) and 1(e). The phase accumulation along the x direction for a fixed transverse momentum is proportional to $(k^+_{e,\uparrow} - k^-_{e,\uparrow} + k^-_{h,\downarrow} - k^+_{h,\downarrow})L$ where L is the width of the AM interlayer. Due to the distinct band splitting, the phase accumulation is enhanced by $d_{x^2-y^2}$-AM order but largely vanishes for d_{xy}-AM order. Thus, the resonant states can be formed in the short junction with $d_{x^2-y^2}$-AM order and the oscillatory transport behavior can thus be expected. Interestingly, we found that the phase accumulation also affects the formation of surface Andreev bound states, which are vulnerable to the $d_{x^2-y^2}$-AM order but almost immune to the d_{xy}-AM order, though the time-reversal symmetries are broken for both cases. Second, we investigate the Josephson effect of the d-SC/AM/d-SC Josephson junction as shown in Fig. 1(b). We calculate the Josephson current $I(\varphi)$ for various orientations of the junctions where φ is the macroscopic phase difference between two d-SCs. We obtain the altermagnetism-induced 0-π transitions in symmetric junctions. In the case of $d_{x^2-y^2}$-SC/AM/d_{xy}-SC junction, where the first order of Josephson current is absent without AM [68,69], we find that the first-order Josephson coupling reemerges when AM is neither $d_{x^2-y^2}$ nor d_{xy} wave. We further provide the explanation of our numerical results by symmetry analysis.

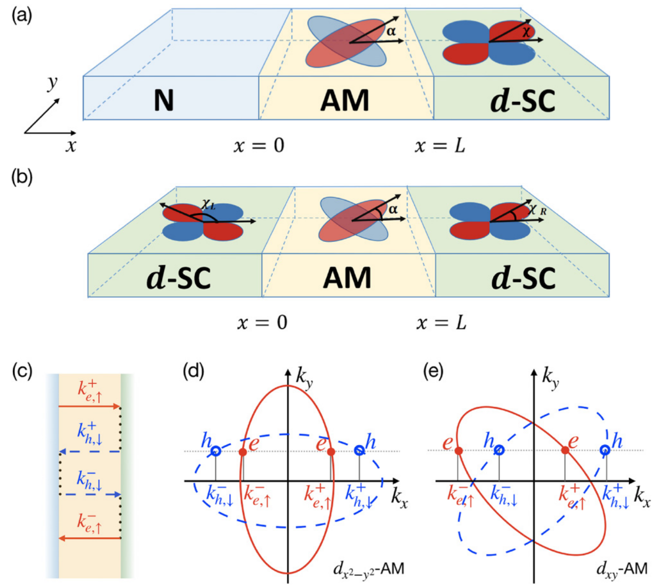

FIG. 1. Schematics of (a) the normal metal (N)/altermagnet (AM)/d-wave superconductor (d-SC) junction and (b) the d-SC/AM/d-SC junction. (c) Sequential transport processes inside AM interlayer which are necessary to form de Gennes-Saint-James states. Solid line stands for electron and dashed line stands for hole. (d) For the $d_{x^2-y^2}$-AM case, band splitting enhances phase accumulation $(k^+_{e,\uparrow} - k^-_{e,\uparrow} + k^-_{h,\downarrow} - k^+_{h,\downarrow})L$ and thus the resonant states can be generated with small L. Such phase accumulation is almost zero for the d_{xy}-AM case (e) and no resonant state can be formed in the short junction.

The paper is organized as follows: In Sec. II, we introduce our model and formalism. In Sec. III, we show numerical results for N/AM/d-SC junctions and discuss the orientation dependence of forming resonant states. In Sec. IV, we show the Josephson effect in d-SC/AM/d-SC junctions. Our conclusions are given in Sec. V.

II. MODEL AND FORMALISM

In this section, we provide a formulation to calculate conductance and Josephson current using the scattering approach. As depicted in Figs. 1(a) and 1(b), we consider N/AM/d-SC and d-SC/AM/d-SC junctions which are translation invariance in the y direction. $\hat{H}$ corresponds to the Hamiltonian of low-energy excitations

$$\hat{H} = \begin{pmatrix} H_0 & \hat{\Delta} \\ \hat{\Delta} & -H_0^* \end{pmatrix}, \hat{\Delta} = i\hat{\sigma}_y \Delta, \tag{1}$$

$$H_0 = \frac{\hbar^2 \mathbf{k}^2}{2m} + U - \mu + \mathcal{M}\hat{\sigma}_z, \tag{2}$$

in the basis $(\psi_\uparrow, \psi_\downarrow, \psi^\dagger_\uparrow, \psi^\dagger_\downarrow)^T$. Δ is the position-dependent d-wave pairing potential. The wave vector $\mathbf{k}$ is given by $\mathbf{k} = (k_x, k_y)$ and μ is the uniform chemical potential so that the Fermi wave vector is $k_F = \sqrt{2m\mu}/\hbar$, with m the electron mass. U is the barrier potential $U(x) = U_1\delta(x) + U_2\delta(x-L)$ and we define dimensionless parameters $Z_{1(2)} = mU_{1(2)}/(\hbar^2 k_F)$. $\hat{\sigma}_{i=x,y,z}$ are Pauli matrices in the spin space. $\mathcal{M}$ denotes the exchange potential of altermagnet and without loss of generality, the Néel vector of AM is along the z axis,

$$\mathcal{M} = \left[\frac{J_1}{2}\left(k_x^2 - k_y^2\right) + J_2 k_x k_y\right]\Theta(x)\Theta(L-x), \tag{3}$$

with Θ being the Heaviside function, $J_1 = 2Jk_F^{-2}\sin 2\alpha$, $J_2 = 2Jk_F^{-2}\cos 2\alpha$, and J the strength of the exchange energy of the AM. The junction length is L . We denote α the angle between the lobe of the direction of the altermagnet and the x axis. For $\alpha = 0$, the magnetization has pure $d_{x^2-y^2}$-wave symmetry and for $\alpha = \pi/4$, it has pure d_{xy}-wave symmetry.

To find the conductance and Josephson current, we construct the wave functions in each region of the junction.

In the N/AM/d-SC junction as shown in Fig. 1(a), Δ is given by

$$\Delta = \Delta_0 \cos(2\theta - 2\chi)\Theta(x-L), \tag{4}$$

where θ is the propagating angle in superconductors of quasiparticles with $k_y = k_F\sin\theta$. The quantity χ is taken to be the angle of the positive d-wave lobe with respect to the interface normal. We denote $\psi_{1(2)}$ for wave functions as an incident spin-↑ (↓) electron with energy E injects from the normal side. Due to the translational invariance along the y axis, the transverse momentum k_y is conserved. On the normal side, we have

$$\psi_{1(2)}(x \leqslant 0) = (e^{ik^+x}\check{e}_{1(2)} + a_{1(2)}e^{ik^-x}\check{e}_{4(3)} + b_{1(2)}e^{-ik^+x}\check{e}_{1(2)})e^{ik_y y}. \tag{5}$$

Here, we denote $k^\pm = \sqrt{2m(\mu \pm E)/\hbar^2 - k_y^2}$ as the wave vectors for electrons (+) and holes (–), and a_i and b_i are the coefficients of reflected waves. We define $\check{e}_1 = (1,0,0,0)^T$, $\check{e}_2 = (0,1,0,0)^T$, $\check{e}_3 = (0,0,1,0)^T$, and $\check{e}_4 = (0,0,0,1)^T$ as basis functions. In the middle AM region, we have

$$\psi_{1(2)}(0<x<L) = (w_{1(\bar{1})}e^{ik^+_{e,\uparrow(\downarrow)}x}\check{e}_{1(2)} + w_{2(\bar{2})}e^{ik^-_{e,\uparrow(\downarrow)}x}\check{e}_{1(2)} + w_{3(\bar{3})}e^{ik^+_{h,\downarrow(\uparrow)}x}\check{e}_{4(3)} + w_{4(\bar{4})}e^{ik^-_{h,\downarrow(\uparrow)}x}\check{e}_{4(3)})e^{ik_y y}, \tag{6}$$

with wave vectors

$$k^\pm_{e,s} = \pm\frac{\hbar}{\hbar^2 + p_s mJ_2}\sqrt{2m(\mu+E)\left(1+\frac{mJ_2}{\hbar^2}\right) - \hbar^2k_y^2 + \frac{m^2\left(J_1^2+J_2^2\right)k_y^2}{\hbar^2}} - \frac{p_s mJ_1k_y}{\hbar^2 + p_s mJ_2}, \tag{7}$$

$$k^\pm_{h,s} = \pm\frac{\hbar}{\hbar^2 + p_s mJ_2}\sqrt{2m(\mu-E)\left(1+\frac{mJ_2}{\hbar^2}\right) - \hbar^2k_y^2 + \frac{m^2\left(J_1^2+J_2^2\right)k_y^2}{\hbar^2}} - \frac{p_s mJ_1k_y}{\hbar^2 + p_s mJ_2}. \tag{8}$$

Here, we define $p_{s=\uparrow} = +1$ and $p_{s=\downarrow} = -1$, while w_i and $w_{\bar{i}}$ are the coefficients of scattering waves. On the superconducting side, the wave functions are given by

$$\psi_{1(2)}(x \geqslant L) = (f_{1(\bar{1})}e^{iq^+x}\check{e}_{1(2)} \pm f_{1(\bar{1})}\gamma_1 e^{iq^+x}\check{e}_{4(3)} + g_{1(\bar{1})}\gamma_2 e^{-iq^-x}\check{e}_{1(2)} \pm g_{1(\bar{1})}e^{-iq^-x}\check{e}_{4(3)})e^{ik_y y}, \tag{9}$$

where the wave vectors are $q^\pm = \sqrt{2m(\mu \pm \sqrt{E^2-\Delta^2})/\hbar^2 - k_y^2}$, and f_1, $f_{\bar{1}}$, g_1, and $g_{\bar{1}}$ are the coefficients. The coherence factors γ_1 and γ_2 are as follows [19]:

$$\gamma_1 = \frac{\Delta(T)\cos(2\theta-2\chi)}{E + \sqrt{E^2 - \Delta(T)^2\cos^2(2\theta-2\chi)}}, \quad \gamma_2 = \frac{\Delta(T)\cos(2\theta+2\chi)}{E + \sqrt{E^2 - \Delta(T)^2\cos^2(2\theta+2\chi)}}. \tag{10}$$

The scattering coefficients are determined by continuity of wave functions $\psi|_{x=0^+} = \psi|_{x=0^-}$, $\psi|_{x=L^+} = \psi|_{x=L^-}$ and

$$\left(\frac{\hbar^2}{m} + J_2\hat{\sigma}_z\right)\partial_x\psi|_{x=0^+} - \frac{\hbar^2}{m}\partial_x\psi|_{x=0^-} = (-iJ_1k_y\hat{\sigma}_z + 2U_1)\psi|_{x=0}, \tag{11}$$

$$\frac{\hbar^2}{m}\partial_x\psi|_{x=L^+} - \left(\frac{\hbar^2}{m} + J_2\hat{\sigma}_z\right)\partial_x\psi|_{x=L^-} = (iJ_1k_y\hat{\sigma}_z + 2U_2)\psi|_{x=L}. \tag{12}$$

As a result, we can utilize the Blonder-Tinkham-Klapwijk (BTK) formalism [19,70–72] to compute the differential conductance

$$\sigma/\sigma_0 = \int_{-\pi/2}^{\pi/2}\sigma(\theta)\cos\theta d\theta \Big/ \int_{-\pi/2}^{\pi/2}\sigma_0(\theta)\cos\theta d\theta, \tag{13}$$

with $\sigma(\theta) = 2 + |a_1|^2 + |a_2|^2 - |b_1|^2 - |b_2|^2$. Here, σ_0 denotes the conductance when the superconductor is in the normal state $\sigma_0(\theta) = 2 - |b_{N1}|^2 - |b_{N2}|^2$, and $b_{N1(2)}$ is the corresponding scattering coefficient for the spin-↑ (↓) electron reflection.

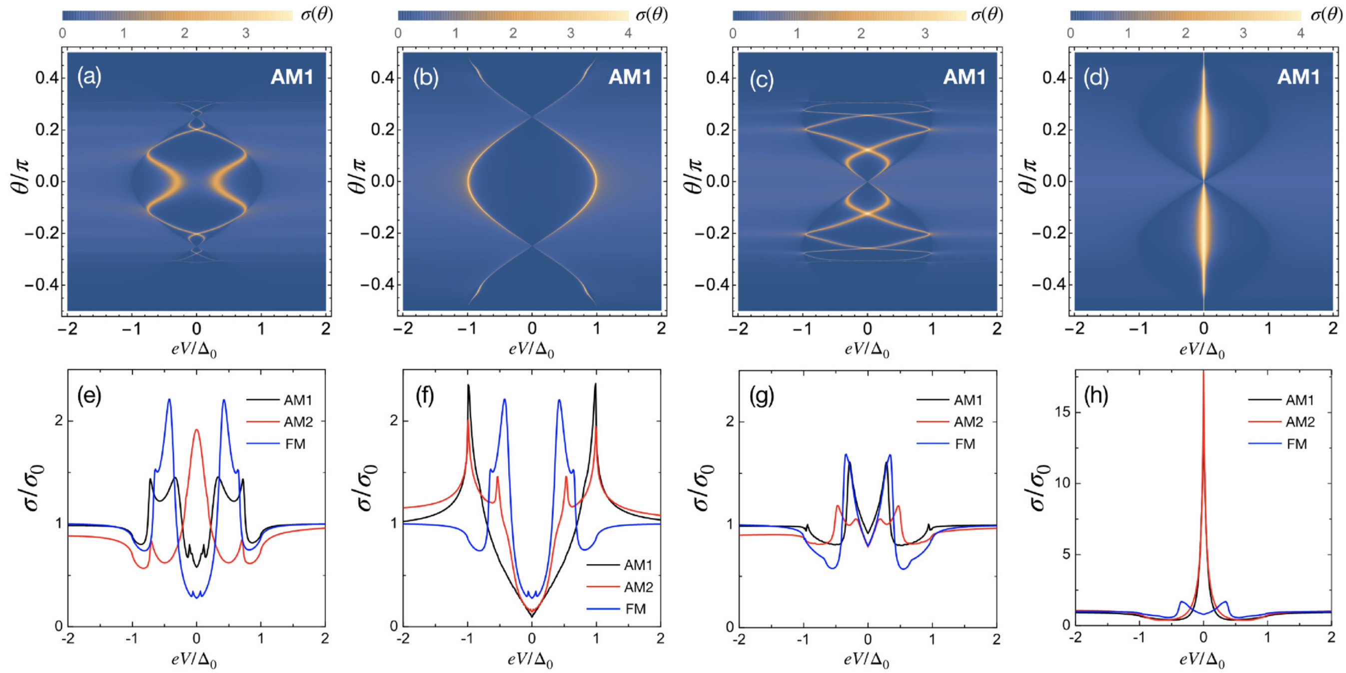

FIG. 2. Tunneling conductance. AM1 (AM2) stands for the N/AM/SC junction in the case of $Z_2 = 0$ ($Z_2 = 0.5$). FM stands for the N/ferromagnet/SC junction with $Z_2 = 0$. (a)–(d) Angle-resolved conductance $\sigma(\theta)$ of AM1 geometry. (e)–(h) The normalized conductance σ/σ_0 of AM1 (black), AM2 (red), and FM (blue). We set $k_F L = 10$, $\Delta_0 = 0.01\mu$, $Z_1 = 2$ for all panels. The altermagnetic strength is $J/\mu = 0.2$ in the AM1 and AM2 junction. The exchange field in the FM junction is $M = 0.5\mu$. The superconductor has $d_{x^2-y^2}$-wave symmetry ($\chi = 0$) in panels (a), (b), (e), and (f) and has d_{xy}-wave symmetry ($\chi = \pi/4$) in panels (c), (d), (g), and (h). The altermagnetic orders of AM1 and AM2 have the $d_{x^2-y^2}$-wave symmetry ($\alpha = 0$) in panels (a), (c), (e), and (g) and d_{xy}-wave symmetry ($\alpha = \pi/4$) in panels (b), (d), (f), and (h).

For the d-SC/AM/d-SC Josephson junction as shown in Fig. 1(b), the pair potential is given by [69,73–75]

$$\Delta(x) = \begin{cases} \Delta(T)\cos(2\theta - 2\chi_L)e^{i\varphi}, & x < 0, \\ 0, & 0 < x < L, \\ \Delta(T)\cos(2\theta - 2\chi_R), & x > L. \end{cases} \quad (14)$$

Here, φ is the macroscopic phase difference between the left and right superconductors and χ_L and χ_R are the angles of the positive d-wave lobe on the left and right side, respectively. The pair potential at zero temperature $\Delta(T=0)$ is still Δ_0 and its temperature dependence is determined by mean-field approximation [69,74]. We focus on the Josephson effect in the low temperature limit in this paper. Now, we can solve wave functions of each region for the scattering processes. By using the standard Furusaki-Tsukada's formula [69,74,76], we obtain the Josephson current

$$I = \int_{-\pi/2}^{\pi/2} \frac{ek_BT}{2\hbar} \sum_{\omega_n, s=\uparrow,\downarrow} \left(\frac{\Delta(T)\cos(2\theta - 2\chi_L)a_{he,s}}{\sqrt{\omega_n^2 + \Delta^2(T)\cos^2(2\theta - 2\chi_L)}} - \frac{\Delta(T)\cos(2\theta + 2\chi_L)a_{eh,s}}{\sqrt{\omega_n^2 + \Delta^2(T)\cos^2(2\theta + 2\chi_L)}} \right) \cos\theta d\theta, \quad (15)$$

with $a_{he,s}$ ($a_{eh,s}$) being the coefficient of Andreev reflection from incident electron (hole) to reflected hole (electron) with spin s. Here, we have made analytical continuation of incident quasiparticle energy $E \to i\omega_n$ into Matsubara frequencies $\omega_n = \pi k_B T(2n+1)$, $(n = 0, \pm1, \pm2....)$. Equation (15) allows us to directly calculate the dc Josephson current in even more complicated or long junctions, but we will focus on the short junction with $k_F L \ll \mu/\Delta$ in this work.

III. IDENTIFICATION OF DE GENNES-SAINT-JAMES STATES VIA CONDUCTANCE

First, we show the angle-resolved conductance $\sigma(\theta)$ and the normalized conductance σ/σ_0 of N/AM/d-SC junctions in Fig. 2 using Eq. (13). To observe the resonant states, we require a finite barrier strength between N and AM (we set $Z_1 = 2$), which can confine the quasiparticle transport inside the AM. For a d-wave superconductor, e.g., yttrium barrium copper oxide YBCO, a representative choice would be $\Delta_0 \approx 10-20$ meV, and $\mu \approx 1$ eV [77] so that we can estimate $\Delta_0 = 0.01\mu$. The length of the AM layer is set to $k_F L = 10$, which experimentally relates to the short junction limit $k_F L \ll \mu/\Delta_0$. We first consider the case of no barrier ($Z_2 = 0$) at the right interface between AM and d-SC (AM1 geometry). For altermagnets, the spin-splitting is nonrelativistic and it can reach several hundred meV [43] and here we first choose $J/\mu = 0.2$ in Fig. 2. From Figs. 2(a) and 2(c) we can see that there are subgap resonance spikes when the altermagnetic order has $d_{x^2-y^2}$-wave symmetry, indicating the formation of de Gennes-Saint-James states. As a result, the characteristic subgap resonance peaks show up in the normalized differential conductance σ/σ_0, see the black lines in Figs. 2(e) and 2(g). In comparison, a short d_{xy}-AM can not produce resonant states or the resonance spikes in the angle-resolved conductance spectra as shown in Figs. 2(b) and 2(d). Instead, we found the well-known V-shape conductance and the zero-biased conductance peak for $d_{x^2-y^2}$-SC and d_{xy}-SC, respectively, see the black lines in Figs. 2(f) and 2(h). We now consider a finite barrier between AM and d-SC, that is, $Z_2 \neq 0$ (AM2 geometry) plotted with red lines in Fig. 2. The presence of the second barrier does not qualitatively change the dependence on the altermagnet orientation of the resonant states. Such induced resonant states have strong dependence on k_y and when the dispersion $E(k_y)$ is almost flat across a certain range of k_y, the resonant peak in the conductance σ clearly appears. It is also worth noting that there are similarities between ferromagnet [29] and $d_{x^2-y^2}$-AM in terms of the ability to generate de Gennes-Saint-James states as a result of their band splittings. For a junction featuring a FM instead of an AM (FM geometry), we plot the N/FM/SC conductance with the ferromagnetic exchange field $M = 0.5\mu$ [78,79] with blue lines in Fig. 2. For both pairing states, there are subgap resonant spikes in the spectra.

The previous results are explained through a resonance condition for the emergence of Andreev states in the intermediate AM region. That is, resonances form when the phase accumulated after scattering on the left and right interfaces of the intermediate AM region is a multiple of 2π. We now show how the phase accumulated is greatly influenced by the symmetry of the AM order. First, we look at the phase accumulation by the Andreev reflections at the right interface between altermagnet and d-wave superconductor (for simplicity, we consider the $Z_2 = 0$ case). For a semi-infinite AM/d-wave SC junction, we obtain the coefficients $r_{h\downarrow,e\uparrow}$, $r_{h\uparrow,e\downarrow}$, $r_{e\uparrow,h\downarrow}$, and $r_{e\downarrow,h\uparrow}$ corresponding to the Andreev reflection probability amplitudes of the spin-up incident electron, the spin-down incident electron, the spin-down incident hole, and the spin-up incident hole, respectively. Specifically,

$$r_{h\downarrow,e\uparrow(h\uparrow,e\downarrow)} = \frac{\pm 2[k^+_{e,\uparrow(\downarrow)} - k^-_{e,\uparrow(\downarrow)}]k_x(1 \pm \tilde{\alpha}_2)}{[\Omega_{1(2)}\gamma_1\gamma_2 - \Xi_{1(2)}]\gamma_1^{-1}}, \quad (16a)$$

$$r_{e\uparrow,h\downarrow(e\downarrow,h\uparrow)} = \frac{\pm 2[k^+_{h,\downarrow(\uparrow)} - k^-_{h,\downarrow(\uparrow)}]k_x(1 \mp \tilde{\alpha}_2)}{[\Omega_{1(2)}\gamma_1\gamma_2 - \Xi_{1(2)}]\gamma_2^{-1}}, \quad (16b)$$

with

$$\Xi_{1(2)} = \big[\Lambda^e_{1(2)} - k_x\big]\big[\Lambda^h_{1(2)} + k_x\big], \quad (17a)$$

$$\Omega_{1(2)} = \big[\Lambda^e_{1(2)} + k_x\big]\big[\Lambda^h_{1(2)} - k_x\big], \quad (17b)$$

$$\Lambda^e_{1(2)} = (1 \pm \tilde{\alpha}_2)k^-_{e,\uparrow(\downarrow)} \pm \tilde{\alpha}_1 k_y, \quad (17c)$$

$$\Lambda^h_{1(2)} = (1 \mp \tilde{\alpha}_2)k^+_{h,\downarrow(\uparrow)} \mp \tilde{\alpha}_1 k_y. \quad (17d)$$

Here, $\tilde{\alpha}_{1(2)}$ denotes the dimensionless AM strength $\tilde{\alpha}_{1(2)} = mJ_{1(2)}/\hbar^2$ and we assume that $|\tilde{\alpha}_{1(2)}| < 1$ to have a well-defined Fermi surface. The wave vector k_x is given by $k_x = \sqrt{k_F^2 - k_y^2}$. When the propagating spin-up electron or spin-down hole undergo sequential Andreev reflections at the interface of our system, the gained phase is the argument of $r_{e\uparrow,h\downarrow}r_{h\downarrow,e\uparrow}$, with

$$r_{e\uparrow,h\downarrow}r_{h\downarrow,e\uparrow} = \frac{4(k^+_{h,\downarrow} - k^-_{h,\downarrow})(k^+_{e,\uparrow} - k^-_{e,\uparrow})k_x^2\big(1 - \tilde{\alpha}_2^2\big)}{(\Omega_1\gamma_1\gamma_2 - \Xi_1)^2\gamma_1^{-1}\gamma_2^{-1}}. \quad (18)$$

First, we consider a $d_{x^2-y^2}$-wave superconducting pairing, where $\gamma_1 = \gamma_2$ is expected. When the energy E is at the band edge $E = -|\Delta_+|$ ($E = |\Delta_+|$), $\gamma_{1(2)}$ takes the value $\gamma_1 = \gamma_2 = -1(+1)$. Moreover, we have $\gamma_1 = \gamma_2 = -i$ at zero energy. Therefore, as E varies inside the energy gap, the accumulated phase due to sequential Andreev reflections, ϕ_{AR}, is a value between -2π and 0. A $d_{x^2-y^2}$-AM can give rise to a finite phase $\phi_{AM} = (k^+_{e,\uparrow} - k^-_{e,\uparrow} + k^-_{h,\downarrow} - k^+_{h,\downarrow})L$ together with a phase ϕ_N from the normal reflections at the interface between N and AM. As a result, it is possible to fulfill the Bohr-Sommerfeld condition for the formation of an Andreev bound state,

$$\phi_{AR} + \phi_{AM} + \phi_N = 2\pi m, \quad (19)$$

where m is an integer. For finite k_y, there could be another phase accumulation along the y axis for the $d_{x^2-y^2}$-AM case but it would not affect our conclusions.

On the other hand, a d_{xy}-AM makes $\phi_{AM} \approx 0$ for a short L. Moreover, in the heavily doped regime with $E \ll \mu$, the normal reflection coefficients at the N/d_{xy}-AM interface become

$$r_{e\uparrow} = r^*_{h\downarrow} = \frac{q - k_x - 2iZ_1k_F}{q + k_x + 2iZ_1k_F}, \quad (20)$$

with

$$q = \sqrt{\frac{2m\mu}{\hbar^2} - k_y^2 + \tilde{\alpha}_1^2 k_y^2}. \quad (21)$$

The phase accumulation ϕ_N taken from $r_{e\uparrow}$ and $r_{h\downarrow}$ is zero, and Eq. (19) reduces to $\phi_{AR} + \phi_{AM} + \phi_N \approx \phi_{AR} \in (-2\pi, 0)$, which is insufficient to form Andreev bound states.

We now use a similar reasoning to analyze the d_{xy}-wave pairing states, where the relation between γ_1 and γ_2 changes to $\gamma_1 = -\gamma_2$. Consequently, ϕ_{AR} belongs to the range $(-\pi, \pi)$ for subgap energies and at zero energy we have $\phi_{AR} = 0$. This indicates that the surface flat bands characteristic of d_{xy} pairing are robust against the presence of d_{xy}-AM since the Bohr-Sommerfeld condition [80], Eq. (19), is always satisfied at $E = 0$, i.e., $\phi_{AR} + \phi_{AM} + \phi_N \approx \phi_{AR} = 0$. However, for a $d_{x^2-y^2}$-AM, $\phi_{AM} + \phi_N$ does not vanish and the expected Andreev bound states can exist inside the gap for $E \neq 0$.

To see the dependence of the resonant states on the strength of the AM, we show the density plot of the conductance spectra as a function of eV and altermagnetic strength J in Figs. 3(a)–3(d). Figures 3(a) and 3(c) show that, with the increase of the strength of altermagnetism J, the oscillatory conductance spikes emerge if AM has $d_{x^2-y^2}$-wave order. Specifically, there are more subgap spikes for the $d_{x^2-y^2}$ -SC junction than for the d_{xy}-SC junction for large values of J. This indicates that $d_{x^2-y^2}$-AM order mainly suppresses the flat zero-energy states in the d_{xy}-SC junctions. However, if the AM has d_{xy}-wave order, the characteristic of tunneling spectra is invariant as compared to the junction without AM, as seen in Figs. 3(b) and 3(d). We further show the effect of the junction length on the emergence of resonant states. Figures 3(e)–3(h) show that the number of spikes is proportional to L since the phase accumulation increases with L. As expected, the resonant states can be generated for the $d_{x^2-y^2}$-wave AM order in the short junction [Figs. 3(e) and 3(g)], but can only be found for the d_{xy}-wave AM order in the long junction limit [$k_FL > 10^3$, see Figs. 3(f)–3(h)], because of the negligible difference between electron and hole wave vectors. We note that the height of the subgap resonant spikes tends to be suppressed as L increases in Fig. 3(e). The dispersion of the bound states $E(\theta)$ must become almost flat

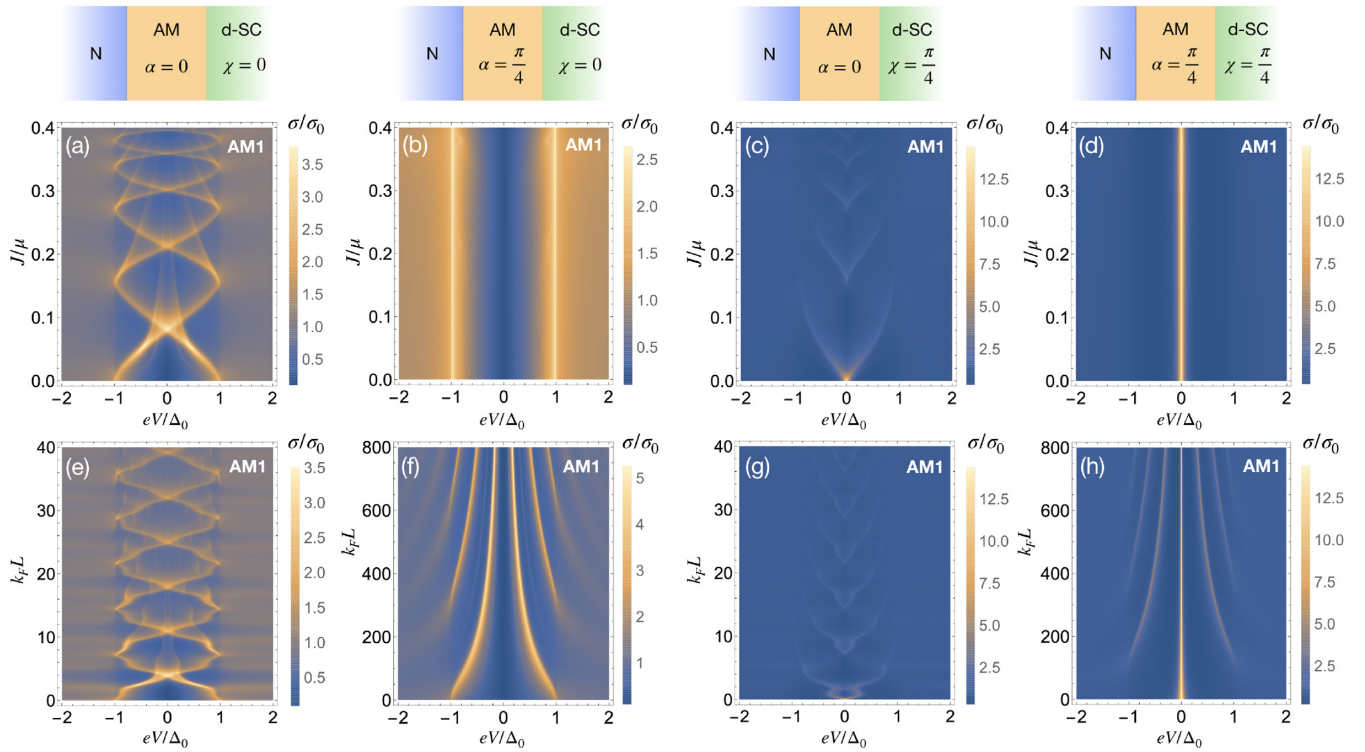

FIG. 3. Parameter dependence of conductance of the AM1 geometry. (a)–(d) conductance varies with J and eV for $k_F L = 10$. (e)–(h) conductance varies with L and eV for $J/\mu = 0.2$. The AM order is $d_{x^2-y^2}$ for (a), (c), (e), and (g) and d_{xy} for (b), (d), (f), and (h). The pairing symmetry of SC is $d_{x^2-y^2}$ for (a), (b), (e), and (f) and d_{xy} for (c), (d), (g), and (h). The barriers in the AM1 case are $Z_1 = 2$ and $Z_2 = 0$ for all panels.

across a certain range of $\theta \in (\theta_l, \theta_u)$ to form the resonant conductance peak, see also the numerical results in Figs. 2(a) and 2(e). The reason for this is that the density of the resonant states is particularly high for energies where quasiflat bands appear. As the junction length L increases, more resonant states are induced and their dispersions depend more sensitively on the incident angle θ, thus the range of quasiflat band region $(\theta_u - \theta_l)$ becomes smaller and the quasiflat bands have reduced density of states at large L. It is worthwhile to point out that de Gennes-Saint-James states have already been shown in the AM/AM/SC junction without unconventional pair potential [56] and thus found to be absent in semi-infinite AM/SC system [55] since the resonant states come from the confinement effect [81].

IV. THE JOSEPHSON EFFECT

In this section, we discuss the current phase relation (CPR) $I(\varphi)$ in d-SC/AM/d-SC junctions, where φ is the phase difference between the left and the right pair potentials. We set equal barriers at left and right interfaces ($Z_1 = Z_2 = Z$) between AM and SC. Scattering coefficients are calculated numerically by imposing boundary conditions for the scattering wave functions, and the Josephson current is obtained by Eq. (15).

To analyze the CPR, we further decompose the Josephson current into a series of different orders of Josephson coupling

$$I(\varphi) = \sum_n [I_n \sin(n\varphi) + J_n \cos(n\varphi)], \tag{22}$$

where n is a positive integer. We consider different parameters such as the crystal orientation $\chi_{L,R}$, α and find that the CPR is expressed as $\sum_n I_n \sin(n\varphi)$ and J_n is zero in our system. To demonstrate this, a relevant operator is the fourfold rotation symmetry C_4 which corresponds to a rotation angle $\pi/2$ with respect to the z axis and makes $k_x \to k_y$, $k_y \to -k_x$, $\hat{s}_z \to \hat{s}_z$, and φ invariant. Another relevant operator is the time-reversal symmetry T, which induces the transformations $k_x \to -k_x$, $k_y \to -k_y$, $\hat{s}_z \to -\hat{s}_z$, and $\varphi \to -\varphi$. We consider the combined symmetry $M_0 = TC_4$ [64] which is maintained in the system,

$$M_0 \hat{H}(\varphi) M_0^{-1} = \hat{H}(-\varphi). \tag{23}$$

Consequently, the Josephson current satisfies the well-known characteristic $I(\varphi) = -I(-\varphi)$ with symmetry protected zero net current at $\varphi = 0$ or π, indicating that $J_n \cos(n\varphi)$ must vanish in the CPR of our Josephson junction.

Figure 4 shows the Josephson current in $d_{x^2-y^2}$-SC/AM/$d_{x^2-y^2}$-SC junctions with various crystal orientations of the AM. It can be seen that the altermagnetic strength J can drive the $0-\pi$ transitions. Moreover, high-order Josephson coupling can be dominant in this geometry, for example, the black curve in Fig. 4(a). We also find the anomalous skewness in the CPR, e.g., the red curve in Fig. 4(a) and the black curve in Fig. 4(d). Comparing to the upper panels (a)–(c) with lower panels (d)–(f), one can see that the $0-\pi$ transition can occur when the junction length varies, for example, the black curves in (b) and (e). The feature of Josephson current is also sensitive to the crystal orientation α of the AM, that is, α can also drive the $0-\pi$ transition when other parameters

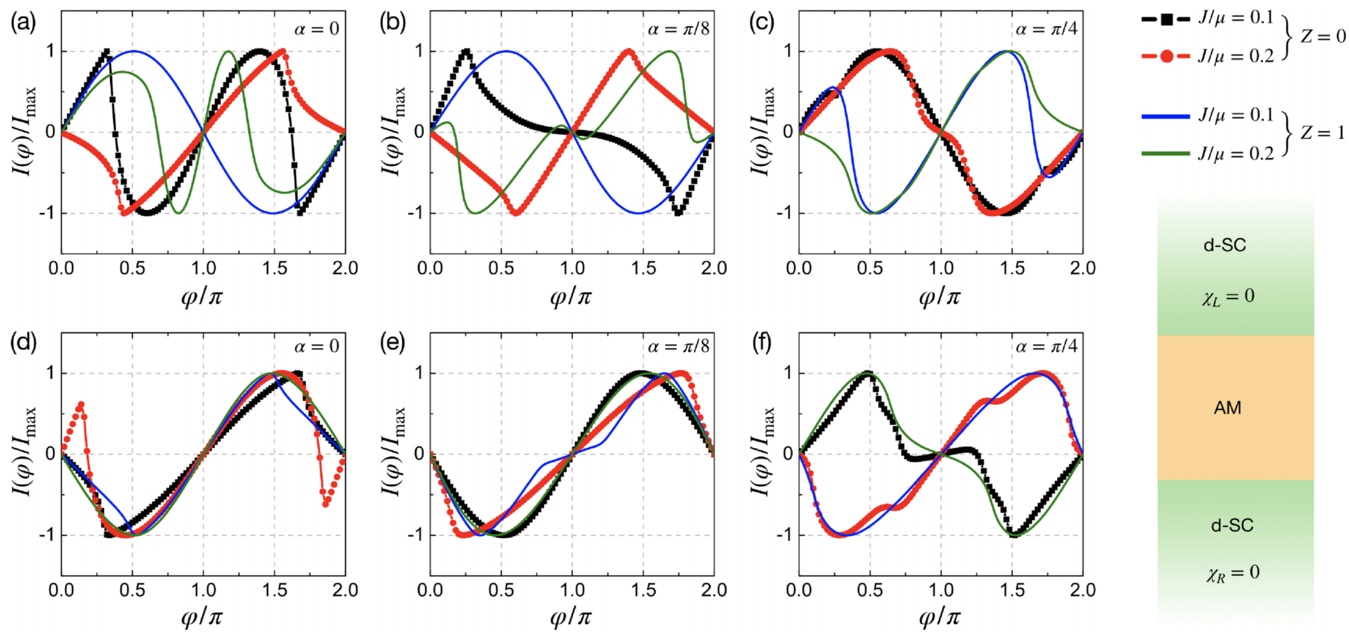

FIG. 4. Current phase relation of $d_{x^2-y^2}$-SC/AM/$d_{x^2-y^2}$-SC Josephson junction. (a)–(c) $k_F L = 10$ and (d)–(f) $k_F L = 20$. We choose the temperature $k_B T = 0.01084\Delta_0$. The current I has been normalized to the critical current $I_{\max} = \max[I(\varphi)]$. The value of Z is zero for black and red curves and is one for blue and green curves.

are kept the same. We find a similar behavior of the CPR in a d_{xy}-SC/AM/d_{xy}-SC junction. The presence of a finite barrier $Z \neq 0$ does not break M_0 symmetry and, therefore, would not qualitatively alter the current-phase characteristics, see blue and green curves in Fig. 4.

We next show the CPR in asymmetric $d_{x^2-y^2}$-SC/AM/d_{xy}-SC junctions in Fig. 5. For $d_{x^2-y^2}$-AM, the second order Josephson coupling is dominant but the sign of I_2 is highly tunable by the strength of altermagnetism as shown in Figs. 5(a) and 5(d). It is also noted that the current at phase difference $\varphi = \pm\pi/2$ becomes zero. Such behavior is the same with the case without magnetization. To explain the nodal point at $\varphi = \pm\pi/2$, we consider the mirror reflection with respect to the xz plane M_{xz}, which makes $k_x \to k_x$, $k_y \to -k_y$, $\hat{s}_z \to -\hat{s}_z$, and additional phase $\varphi \to \varphi - \pi$. We use the magnetic mirror reflection symmetry $M_1 = TM_{xz}$ [82,83], which leads to $k_x \to -k_x$, $k_y \to k_y$, $\hat{s}_z \to \hat{s}_z$, and $\varphi \to -\varphi + \pi$. We

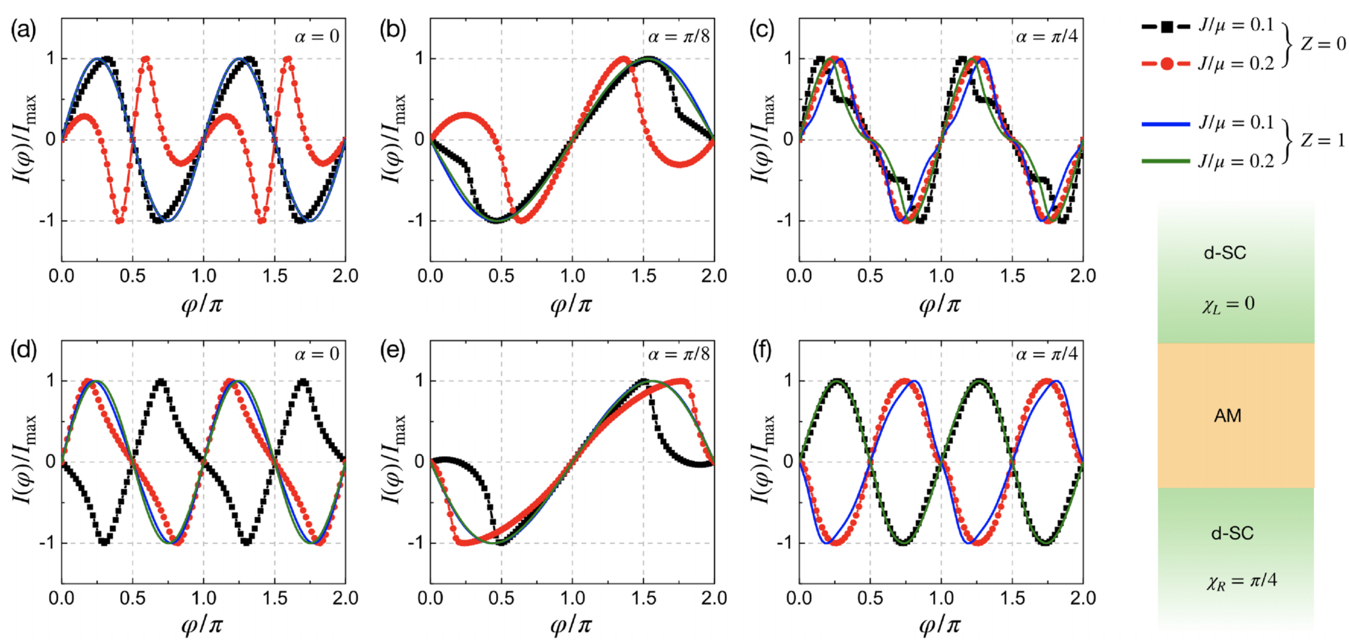

FIG. 5. Current phase relation of $d_{x^2-y^2}$-SC/AM/d_{xy}-SC Josephson junction. (a)–(c) $k_F L = 10$ and (d)–(f) $k_F L = 20$. We choose the temperature $k_B T = 0.01084\Delta_0$. The value of Z is zero for black and red curves and is one for blue and green curves.

thus have

$$M_1\hat{H}(\varphi)M_1^{-1} = \hat{H}(-\varphi + \pi) \quad (24)$$

for $d_{x^2-y^2}$-AM. As a result, $-I(-\varphi+\pi) = I(\varphi)$ will be satisfied and we have $I(\varphi = \pm\pi/2) = 0$. It then excludes the presence of odd-order Josephson coupling I_n in the CPR. For d_{xy}-AM, we find a similar feature as compared to $d_{x^2-y^2}$-AM. However, we need to use the complicated combined operator $M_2 = TM_{xz}C_4$ to explain the nodal point at $I(\varphi = \pm\pi/2) = 0$, where M_2 makes $k_x \to k_y$, $k_y \to k_x$, $\hat{s}_z \to \hat{s}_z$, and $\varphi \to -\varphi + \pi$. We arrive at

$$M_2\hat{H}(\varphi)M_2^{-1} = \hat{H}(-\varphi + \pi), \quad (25)$$

for d_{xy}-AM and the system still has vanishing current $I(\varphi = \pm\pi/2) = 0$, as shown in Figs. 5(c) and 5(f). For an AM that is neither $d_{x^2-y^2}$ wave nor d_{xy}-wave, there is no operation that maps $\hat{H}(\varphi)$ to $\hat{H}(-\varphi+\pi)$, and thus the node at $\varphi = \pm\pi/2$ is no longer protected and found to be lifted. Indeed, our numerical results are consistent with our symmetry analysis since the first order Josephson coupling exists for $\alpha = \pi/8$ as shown in Figs. 5(b) and 5(e). As mentioned above, a finite Z would not change the features of the current-phase relation, especially the symmetry-protected vanishing current. We conclude that the CPR, as well as the tunneling conductance, sensitively depends on the orientation of the AM crystal. This is in sharp contrast to the results in $d_{x^2-y^2}$-SC/ferromagnet/d_{xy}-SC junctions where the first-order sinusoidal component never appears in the CPR [84].

V. SUMMARY

In summary, we have theoretically studied the differential conductance and Josephson effect in d-wave altermagnet/d-wave superconductor hybrids. We find that the subgap states, known as de Gennes-Saint-James states, can be enhanced by the $d_{x^2-y^2}$-altermagnet in the short junction but can only be formed in the long junction if the altermagnet has d_{xy}-wave order. We have shown that a robust zero-bias peak against the altermagnetic field can appear when both altermagnetic and superconducting order have d_{xy}-wave symmetry. We further reveal that the 0-π transition can occur in symmetric d-wave Josephson junctions by altermagnetism, which has been widely reported in conventional s-wave Josephson junctions. Notably, we find the orientation-dependent first order Josephson coupling in an asymmetric $d_{x^2-y^2}$-superconductor/altermagnet/d_{xy}-superconductor junction. This feature does not occur in Josephson junctions with d-wave superconductors and ferromagnets, unveiling a unique effect of altermagnetism. Since subgap states are known to promote the formation of odd-frequency spin-triplet Cooper pairs [5,16,85], our results suggest an intriguing possibility for enhancing emerging pair correlations in altermagnets [65,86] and also a powerful way to control them via the Josephson effect. Our findings thus demonstrate the peculiar role of altermagnets on the Josephson effect, of practical significance for both controlling the Josephson current and designing new functional devices in superconducting spintronics.

In terms of material candidates to experimentally test our predictions, it might be possible to exploit the reported d-wave altermagnets [45], such as RuO_2, Mn_5Si_3, or MnO_2. Moreover, recent studies have shown that both the magnetic strength and orientation of altermagnets are electrically controllable [87]. Josephson junctions based on d-wave superconductors with different crystallographic orientations were already reported in high-T_c cuprates [88,89]. Although it may be challenging to continuously tune the orientation angle in experiments as we propose, it might be still possible to examine several discrete angles, avoiding the difficulty of changing pair potentials in one sample. These advances demonstrate that our predictions hold experimental feasibility.

ACKNOWLEDGMENTS

Y.F. acknowledges financial support from the Sumitomo Foundation. P.B. acknowledges support by the Spanish CM "Talento Program" Projects No. 2019-T1/IND-14088 and No. 2023-5A/IND-28927, the Agencia Estatal de Investigación Projects No. PID2020-117992GA-I00 and No. CNS2022-135950, and through the "María de Maeztu" Programme for Units of Excellence in R&D (CEX2023-001316-M). J.C. acknowledges financial support from the Swedish Research Council (Vetenskapsrådet Grant No. 2021-04121) and the Carl Trygger's Foundation (Grant No. 22: 2093). Y.T. acknowledges financial support from JSPS with Grants-in-Aid for Scientific research (KAKENHI Grants No. 23K17668, No. 24K00583, and No. 24K00556). B.L. acknowledges financial support from the National Natural Science Foundation of China (Project 12474049).

DATA AVAILABILITY

The data that support the findings of this article are not publicly available upon publication because it is not technically feasible and/or the cost of preparing, depositing, and hosting the data would be prohibitive within the terms of this research project. The data are available from the authors upon reasonable request.

[1] S. De Franceschi, L. Kouwenhoven, C. Schönenberger, and W. Wernsdorfer, Hybrid superconductor–quantum dot devices, Nat. Nanotechnol. **5**, 703 (2010).

[2] J. Linder and J. W. A. Robinson, Superconducting spintronics, Nat. Phys. **11**, 307 (2015).

[3] S. M. Frolov, M. J. Manfra, and J. D. Sau, Topological superconductivity in hybrid devices, Nat. Phys. **16**, 718 (2020).

[4] E. Prada, P. San-Jose, M. W. A. de Moor, A. Geresdi, E. J. H. Lee, J. Klinovaja, D. Loss, J. Nygård, R. Aguado, and L. P. Kouwenhoven, From Andreev to Majorana bound states in hybrid superconductor–semiconductor nanowires, Nat. Rev. Phys. **2**, 575 (2020).

[5] Y. Tanaka, S. Tamura, and J. Cayao, Theory of Majorana zero modes in unconventional superconductors, Prog. Theor. Exp. Phys. **2024**, 08C105 (2024).

[6] P. G. de Gennes and D. Saint-James, Elementary excitations in the vicinity of a normal metal-superconducting metal contact, Phys. Lett. **4**, 151 (1963).

[7] T. Mizushima and K. Machida, Multifaceted properties of Andreev bound states: interplay of symmetry and topology, Philos. Trans. R. Soc. A **376**, 20150355 (2018).

[8] J. A. Sauls, Andreev bound states and their signatures, Philos. Trans. R. Soc. A **376**, 20180140 (2018).

[9] A. M. Zagoskin, *Quantum Theory of Many-Body Systems* (Springer, New York, 1998).

[10] J. M. Rowell and W. L. McMillan, Electron interference in a normal metal induced by superconducting contracts, Phys. Rev. Lett. **16**, 453 (1966).

[11] J. M. Rowell, Tunneling observation of bound states in a normal metal—superconductor sandwich, Phys. Rev. Lett. **30**, 167 (1973).

[12] S. H. Tessmer, D. J. Van Harlingen, and J. W. Lyding, Observation of bound quasiparticle states in thin Au islands by scanning tunneling microscopy, Phys. Rev. Lett. **70**, 3135 (1993).

[13] C.-R. Hu, Midgap surface states as a novel signature for d^2_{xa}-x^2_b-wave superconductivity, Phys. Rev. Lett. **72**, 1526 (1994).

[14] S. Kashiwaya and Y. Tanaka, Tunnelling effects on surface bound states in unconventional superconductors, Rep. Prog. Phys. **63**, 1641 (2000).

[15] T. Löfwander, V. S. Shumeiko, and G. Wendin, Andreev bound states in high-Tc superconducting junctions, Supercond. Sci. Technol. **14**, R53 (2001).

[16] Y. Tanaka, M. Sato, and N. Nagaosa, Symmetry and topology in superconductors–odd-frequency pairing and edge states–, J. Phys. Soc. Jpn. **81**, 011013 (2012).

[17] S. Kashiwaya, Y. Tanaka, M. Koyanagi, H. Takashima, and K. Kajimura, Origin of zero-bias conductance peaks in high-Tc superconductors, Phys. Rev. B **51**, 1350 (1995).

[18] Y. Tanaka, Y. Tanuma, and A. A. Golubov, Odd-frequency pairing in normal-metal/superconductor junctions, Phys. Rev. B **76**, 054522 (2007).

[19] Y. Tanaka and S. Kashiwaya, Theory of tunneling spectroscopy of d-wave superconductors, Phys. Rev. Lett. **74**, 3451 (1995).

[20] M. Covington, M. Aprili, E. Paraoanu, L. H. Greene, F. Xu, J. Zhu, and C. A. Mirkin, Observation of surface-induced broken time-reversal symmetry in $YBa_2Cu_3O_7$ tunnel junctions, Phys. Rev. Lett. **79**, 277 (1997).

[21] L. Alff, H. Takashima, S. Kashiwaya, N. Terada, H. Ihara, Y. Tanaka, M. Koyanagi, and K. Kajimura, Spatially continuous zero-bias conductance peak on (110) $YBa_2Cu_3O_{7-\delta}$ surfaces, Phys. Rev. B **55**, R14757(R) (1997).

[22] J. Y. T. Wei, N.-C. Yeh, D. F. Garrigus, and M. Strasik, Directional tunneling and Andreev reflection on $YBa_2Cu_3O_{7-\delta}$ single crystals: Predominance of d-wave pairing symmetry verified with the generalized Blonder, Tinkham, and Klapwijk theory, Phys. Rev. Lett. **81**, 2542 (1998).

[23] S. Bouscher, Z. Kang, K. Balasubramanian, D. Panna, P. Yu, X. Chen, and A. Hayat, High-Tc Cooper-pair injection in a semiconductor-superconductor structure, J. Phys.: Condens. Matter **32**, 475502 (2020).

[24] M. Zareyan, W. Belzig, and Y. V. Nazarov, Oscillations of Andreev states in clean ferromagnetic films, Phys. Rev. Lett. **86**, 308 (2001).

[25] E. Vecino, A. Martín-Rodero, and A. Levy Yeyati, Recursion method for nonhomogeneous superconductors: Proximity effect in superconductor-ferromagnet nanostructures, Phys. Rev. B **64**, 184502 (2001).

[26] K. Halterman and O. T. Valls, Proximity effects at ferromagnet-superconductor interfaces, Phys. Rev. B **65**, 014509 (2001).

[27] K. Halterman and O. T. Valls, Proximity effects and characteristic lengths in ferromagnet-superconductor structures, Phys. Rev. B **66**, 224516 (2002).

[28] M. Krawiec, B. L. Györffy, and J. F. Annett, Andreev bound states in ferromagnet-superconductor nanostructures, Physica C: Superconductivity **387**, 7 (2003).

[29] M. Eschrig, Theory of Andreev bound states in SFS junctions and SF proximity devices, Philos. Trans. R. Soc. A **376**, 20150149 (2018).

[30] M. J. M. de Jong and C. W. J. Beenakker, Andreev reflection in ferromagnet-superconductor junctions, Phys. Rev. Lett. **74**, 1657 (1995).

[31] S. Kashiwaya, Y. Tanaka, N. Yoshida, and M. R. Beasley, Spin current in ferromagnet-insulator-superconductor junctions, Phys. Rev. B **60**, 3572 (1999).

[32] I. Žutić and S. Das Sarma, Spin-polarized transport and Andreev reflection in semiconductor/superconductor hybrid structures, Phys. Rev. B **60**, R16322(R) (1999).

[33] C. Visani, Z. Sefrioui, J. Tornos, C. Leon, J. Briatico, M. Bibes, A. Barthélémy, J. Santamaría, and J. E. Villegas, Equal-spin Andreev reflection and long-range coherent transport in high-temperature superconductor/half-metallic ferromagnet junctions, Nat. Phys. **8**, 539 (2012).

[34] M. Naka, S. Hayami, H. Kusunose, Y. Yanagi, Y. Motome, and H. Seo, Spin current generation in organic antiferromagnets, Nat. Commun. **10**, 4305 (2019).

[35] S. Hayami, Y. Yanagi, and H. Kusunose, Momentum-dependent spin splitting by collinear antiferromagnetic ordering, J. Phys. Soc. Jpn. **88**, 123702 (2019).

[36] K.-H. Ahn, A. Hariki, K.-W. Lee, and J. Kuneš, Antiferromagnetism in RuO_2 as d-wave pomeranchuk instability, Phys. Rev. B **99**, 184432 (2019).

[37] M. Naka, S. Hayami, H. Kusunose, Y. Yanagi, Y. Motome, and H. Seo, Anomalous Hall effect in κ-type organic antiferromagnets, Phys. Rev. B **102**, 075112 (2020).

[38] L. Šmejkal, R. González-Hernández, T. Jungwirth, and J. Sinova, Crystal time-reversal symmetry breaking and spontaneous Hall effect in collinear antiferromagnets, Sci. Adv. **6**, eaaz8809 (2020).

[39] S. Hayami, Y. Yanagi, and H. Kusunose, Bottom-up design of spin-split and reshaped electronic band structures in antiferromagnets without spin-orbit coupling: Procedure on the basis of augmented multipoles, Phys. Rev. B **102**, 144441 (2020).

[40] L.-D. Yuan, Z. Wang, J.-W. Luo, E. I. Rashba, and A. Zunger, Giant momentum-dependent spin splitting in centrosymmetric low-z antiferromagnets, Phys. Rev. B **102**, 014422 (2020).

[41] I. I. Mazin, K. Koepernik, M. D. Johannes, R. González-Hernández, and L. Šmejkal, Prediction of unconventional magnetism in doped $FeSb_2$, Proc. Natl. Acad. Sci. USA **118**, e2108924118 (2021).

[42] L. Šmejkal, J. Sinova, and T. Jungwirth, Beyond conventional ferromagnetism and antiferromagnetism: A phase with nonrelativistic spin and crystal rotation symmetry, Phys. Rev. X **12**, 031042 (2022).

[43] L. Šmejkal, J. Sinova, and T. Jungwirth, Emerging research landscape of altermagnetism, Phys. Rev. X **12**, 040501 (2022).

[44] S. Bhowal and N. A. Spaldin, Ferroically ordered magnetic octupoles in d-wave altermagnets, Phys. Rev. X **14**, 011019 (2024).

[45] L. Bai, W. Feng, S. Liu, L. Šmejkal, Y. Mokrousov, and Y. Yao, Altermagnetism: Exploring new frontiers in magnetism and spintronics, Adv. Funct. Mater. **34**, 2409327 (2024).

[46] M. Hu, X. Cheng, Z. Huang, and J. Liu, Catalogue of C-paired spin-momentum locking in antiferromagnetic systems, arXiv:2407.02319.

[47] T. Jungwirth, R. M. Fernandes, J. Sinova, and L. Smejkal, Altermagnets and beyond: Nodal magnetically-ordered phases, arXiv:2409.10034.

[48] R. Tamang, S. Gurung, D. P. Rai, S. Brahimi, and S. Lounis, Newly discovered magnetic phase: A brief review on altermagnets, arXiv:2412.05377.

[49] S.-W. Cheong and F.-T. Huang, Altermagnetism with non-collinear spins, npj Quantum Mater. **9**, 13 (2024).

[50] Y. Fukaya, B. Lu, K. Yada, Y. Tanaka, and J. Cayao, Superconducting phenomena in systems with unconventional magnets, arXiv:2502.15400.

[51] S. Lee, S. Lee, S. Jung, J. Jung, D. Kim, Y. Lee, B. Seok, J. Kim, B. G. Park, L. Šmejkal, C.-J. Kang, and C. Kim, Broken Kramers degeneracy in altermagnetic MnTe, Phys. Rev. Lett. **132**, 036702 (2024).

[52] T. Osumi, S. Souma, T. Aoyama, K. Yamauchi, A. Honma, K. Nakayama, T. Takahashi, K. Ohgushi, and T. Sato, Observation of a giant band splitting in altermagnetic MnTe, Phys. Rev. B **109**, 115102 (2024).

[53] J. Krempaský, L. Šmejkal, S. W. D'Souza, M. Hajlaoui, G. Springholz, K. Uhlířová, F. Alarab, P. C. Constantinou, V. Strocov, D. Usanov, W. R. Pudelko, R. González-Hernández, A. Birk Hellenes, Z. Jansa, H. Reichlová, Z. Šobáň, R. D. Gonzalez Betancourt, P. Wadley, J. Sinova, D. Kriegner *et al.*, Altermagnetic lifting of Kramers spin degeneracy, Nature (London) **626**, 517 (2024).

[54] R. Takagi, R. Hirakida, Y. Settai, R. Oiwa, H. Takagi, A. Kitaori, K. Yamauchi, H. Inoue, J.-i. Yamaura, D. Nishio-Hamane, S. Itoh, S. Aji, H. Saito, T. Nakajima, T. Nomoto, R. Arita, and S. Seki, Spontaneous Hall effect induced by collinear antiferromagnetic order at room temperature, Nat. Mater. **24**, 63 (2025).

[55] C. Sun, A. Brataas, and J. Linder, Andreev reflection in altermagnets, Phys. Rev. B **108**, 054511 (2023).

[56] M. Papaj, Andreev reflection at the altermagnet-superconductor interface, Phys. Rev. B **108**, L060508 (2023).

[57] K. Maeda, B. Lu, K. Yada, and Y. Tanaka, Theory of tunneling spectroscopy in unconventional p-wave magnet-superconductor hybrid structures, J. Phys. Soc. Jpn. **93**, 114703 (2024).

[58] D. Mondal, A. Pal, A. Saha, and T. Nag, Distinguishing between topological Majorana and trivial zero modes via transport and shot noise study in an altermagnet heterostructure Phys. Rev. B **111**, L121401 (2025).

[59] Z. P. Niu and Z. Yang, Orientation-dependent Andreev reflection in an altermagnet/altermagnet/superconductor junction, J. Phys. D **57**, 395301 (2024).

[60] Y. Nagae, A. P. Schnyder, and S. Ikegaya, Spin-polarized specular Andreev reflections in altermagnets Phys. Rev. B **111**, L100507 (2025).

[61] J. A. Ouassou, A. Brataas, and J. Linder, dc Josephson effect in altermagnets, Phys. Rev. Lett. **131**, 076003 (2023).

[62] C. W. J. Beenakker and T. Vakhtel, Phase-shifted Andreev levels in an altermagnet Josephson junction, Phys. Rev. B **108**, 075425 (2023).

[63] S.-B. Zhang, L.-H. Hu, and T. Neupert, Finite-momentum Cooper pairing in proximitized altermagnets, Nat. Commun. **15**, 1801 (2024).

[64] B. Lu, K. Maeda, H. Ito, K. Yada, and Y. Tanaka, φ Josephson junction induced by altermagnetism, Phys. Rev. Lett. **133**, 226002 (2024).

[65] Y. Fukaya, K. Maeda, K. Yada, J. Cayao, Y. Tanaka, and B. Lu, Josephson effect and odd-frequency pairing in superconducting junctions with unconventional magnets, Phys. Rev. B **111**, 064502 (2025).

[66] H.-P. Sun, S.-B. Zhang, C.-A. Li, and B. Trauzettel, Tunable second harmonic in altermagnetic Josephson junctions, Phys. Rev. B **111**, 165406 (2025).

[67] Q. Cheng and Q.-F. Sun, Orientation-dependent Josephson effect in spin-singlet superconductor/altermagnet/spin-triplet superconductor junctions, Phys. Rev. B **109**, 024517 (2024).

[68] S. Yip, Josephson current-phase relationships with unconventional superconductors, Phys. Rev. B **52**, 3087 (1995).

[69] Y. Tanaka and S. Kashiwaya, Theory of Josephson effects in anisotropic superconductors, Phys. Rev. B **56**, 892 (1997).

[70] G. E. Blonder, M. Tinkham, and T. M. Klapwijk, Transition from metallic to tunneling regimes in superconducting microconstrictions: Excess current, charge imbalance, and supercurrent conversion, Phys. Rev. B **25**, 4515 (1982).

[71] T. Fukumoto, K. Taguchi, S. Kobayashi, and Y. Tanaka, Theory of tunneling conductance of anomalous Rashba metal/superconductor junctions, Phys. Rev. B **92**, 144514 (2015).

[72] L. A. B. Olde Olthof, S.-I. Suzuki, A. A. Golubov, M. Kunieda, S. Yonezawa, Y. Maeno, and Y. Tanaka, Theory of tunneling spectroscopy of normal metal/ferromagnet/spin-triplet superconductor junctions, Phys. Rev. B **98**, 014508 (2018).

[73] Y. Tanaka and S. Kashiwaya, Local density of states of quasiparticles near the interface of nonuniform d-wave superconductors, Phys. Rev. B **53**, 9371 (1996).

[74] Y. Tanaka and S. Kashiwaya, Theory of the Josephson effect in d-wave superconductors, Phys. Rev. B **53**, R11957 (1996).

[75] Y. S. Barash, H. Burkhardt, and D. Rainer, Low-temperature anomaly in the Josephson critical current of junctions in d-wave superconductors, Phys. Rev. Lett. **77**, 4070 (1996).

[76] A. Furusaki and M. Tsukada, dc Josephson effect and Andreev reflection, Solid State Commun. **78**, 299 (1991).

[77] J. Linder, T. Yokoyama, and A. Sudbø, Spin-transfer torque and magnetoresistance in superconducting spin valves, Phys. Rev. B **79**, 224504 (2009).

[78] T. Hirai, Y. Tanaka, N. Yoshida, Y. Asano, J. Inoue, and S. Kashiwaya, Temperature dependence of spin-polarized transport in ferromagnet/unconventional superconductor junctions, Phys. Rev. B **67**, 174501 (2003).

[79] Z. Ping Niu and D. Y. Xing, Spin-triplet pairing states in ferromagnet/ferromagnet/d-wave superconductor heterojunctions with noncollinear magnetizations, Phys. Rev. Lett. **98**, 057005 (2007).

[80] M. Sato, Y. Tanaka, K. Yada, and T. Yokoyama, Topology of Andreev bound states with flat dispersion, Phys. Rev. B **83**, 224511 (2011).
[81] J. Cayao and P. Burset, Confinement-induced zero-bias peaks in conventional superconductor hybrids, Phys. Rev. B **104**, 134507 (2021).
[82] A. Yamakage, M. Sato, K. Yada, S. Kashiwaya, and Y. Tanaka, Anomalous Josephson current in superconducting topological insulator, Phys. Rev. B **87**, 100510(R) (2013).
[83] B. Lu, K. Yada, A. A. Golubov, and Y. Tanaka, Anomalous Josephson effect in d-wave superconductor junctions on a topological insulator surface, Phys. Rev. B **92**, 100503(R) (2015).
[84] Y. Tanaka and S. Kashiwaya, Phase dependent energy levels of bound states and D.C. Josephson current in unconventional superconductor / ferromagnetic insulator / unconventional superconductor junctions, J. Phys. Soc. Jpn. **69**, 1152 (2000).
[85] J. Cayao, C. Triola, and A. M. Black-Schaffer, Odd-frequency superconducting pairing in one-dimensional systems, Eur. Phys. J. Spec. Top. **229**, 545 (2020).
[86] K. Maeda, Y. Fukaya, K. Yada, B. Lu, Y. Tanaka, and J. Cayao, Classification of pair symmetries in superconductors with unconventional magnetism Phys. Rev. B **111**, 144508 (2025).
[87] D. Wang, H. Wang, L. Liu, J. Zhang, and H. Zhang, Electric-field-induced switchable two-dimensional altermagnets, Nano Lett. **25**, 498 (2025).
[88] C. C. Tsuei, J. R. Kirtley, C. C. Chi, L. S. Yu-Jahnes, A. Gupta, T. Shaw, J. Z. Sun, and M. B. Ketchen, Pairing symmetry and flux quantization in a tricrystal superconducting ring of $YBa_2Cu_3O_{7-\delta}$, Phys. Rev. Lett. **73**, 593 (1994).
[89] C. C. Tsuei and J. R. Kirtley, Pairing symmetry in cuprate superconductors, Rev. Mod. Phys. **72**, 969 (2000).